Direct Synthesis of Mesoporous Sulfated Silica-Zirconia Catalysts with High Catalytic Activity for Biodiesel via Esterification

Xiao-Rong Chen,[†,‡] Yi-Hsu Ju,[§] and Chung-Yuan Mou*,[†]

Department of Chemistry, National Taiwan University, Taipei 106, Taiwan, College of Chemistry and Chemical Engineering, Nanjing University of Technology, Nanjing 210009, China, and Department of Chemical Engineering, National Taiwan University of Science and Technology, Taipei 106, Taiwan

A solid acid material of high loading of sulfated zirconia on mesoporous silica SBA-15 has been successfully synthesized by a direct-synthesis under strong acidic condition. The materials were characterized by powder X-ray diffraction, N_2 adsorption−desorption, UV−visible diffuse reflectance spectroscopy, transmission electron microscopy (TEM), ICP-mass, and NH_3 temperature-programmed-desorption (TPD). The zirconia content and well-ordered mesostructure of SiO_2−SZ are controllable by tuning the molar ratios of sulfate to zirconia and silica to zirconia. UV−visible spectra and TEM observations confirm the incorporation of zirconium (IV) onto the mesoporoes framework. Acidity is enhanced in comparison with unsupported sulfated zirconia. Much improved catalytic performance under mild temperature condition in the esterification of lauric acid and palmitic acid with the direct-synthesis SiO_2−SZ catalyst was observed as compared to un-supported SZ. The good catalytic performance of the sulfated silica-zirconia materials is attributed to a higher dispersion of zirconia to give higher acid site density and also to better tolerance of water. The solid acid catalytic materials have many advantages over liquid acids in its environmentally friendliness and easy separation.

1. Introduction

Biodiesel is an environmentally friendly fuel as it is made from renewable resources and CO_2 neutral. It is usually derived from the esterification of free fatty acids or the transesterification of triglycerides with methanol or ethanol. In the industrial transesterification process, homogeneous base catalysts, such as sodium and potassium hydroxide, are often used. The base-catalyzed process suffers from some limitations of feedstock. The contents of free fatty acid in the feedstock need to be lower than 0.5 wt %, otherwise soap formation seriously hinders the production of biodiesel.[1,2] Esterification is thus needed for converting long-chain fatty acids into esters.[3,4] Esterifications are conventionally catalyzed homogeneously using concentrated sulfuric acid, which is however corrosive and poor for waste discharge.[5] Solid acid catalysts are preferable, eliminating corrosion problems and offering easy separation of catalysts from the products by filtration.[6] Recently, there have developed various solid acids for the esterification of long chain fatty acids; these include sulfonated carbonized sugar,[7] sulfated zirconia,[8] and organosulfonic acid mesoporous silica.[9] However, the activities of most of these heterogeneous catalysts are still low in comparison with sulfuric acid. It is desirable to further develop good solid acid catalyst with high catalytic activity and stability for the esterification of fatty acid.

There are several considerations in the development of a strong solid acid for the purpose. First, the catalyst needs to be highly dispersed in order to bring out a large number of active acid sites. Second, mesoporosity in the catalyst would be able to accommodate the relatively larger molecules of fatty acid.

Finally, the catalyst needs to be water-tolerant since water is a byproduct of the esterification process.

Previously, Rothenberg and co-workers have screened various solid acids (zeolites, ion-exchange resins, and mixed oxides) for the esterification of fatty acid with methanol at 130−180 °C.[8,10] Under reactive distillation conditions of esterification, there are many advantages in heterogeneous catalysts.[10] They found sulfated zirconia to be the most promising candidate in terms of activity and stability. As a solid acid catalyst, sulfated zirconia offers a number of advantages such as strong acidity and stability which has been extensively exploited in gas-phase catalysis. In our previous works on alkane isomerization, it is known that the catalytic performance can be greatly enhanced by dispersing sulfated zirconia onto mesoporous silica MCM-41.[11] This is because the high surface area of the mesoporous silica provides better dispersion of the solid acid sulfated zirconia and thus provided more acid sites.[11] Mesorosity is especially important in liquid-state catalysis for easy transport of the bulky molecules, such as long chain fatty acids. Mbaraka et al. found that the activity of mesoporous materials functionalized with acidic groups was greatly dependent on the pore dimensions for the esterification of free fatty acids.[12] Liu et al. reported decreasing activity and reusability of catalyst for increasing chain length of carboxylic acid.[13] For the liquid-phase heterogeneous catalytic reaction, the small pore size and poor hydrothermal stabilities of MCM-41 limit its application in esterification of long-chain free fatty acids. It is desirable to have larger pore-size materials as the supports. Mesoporous SBA-15 materials are good candidates as supports for the dispersion of sulfated zirconia because of the properties of their large pore sizes and hydrothermal stabilities.[14]

Postsynthesis is a method usually used for the incorporation of zirconia onto mesoporous silica.[15−17] However, postsynthesis grafting is more cumbersome and may destroy the uniform

---

* Corresponding author. E-mail: cymou@ntu.edu.tw.
† National Taiwan University.
‡ Nanjing University of Technology.
§ National Taiwan University of Science and Technology.

18732 *J. Phys. Chem. C, Vol. 111, No. 50, 2007*

Chen et al.

mesostructure and block the channels. A direct synthesis would be relatively simple and give uniform mesostructure.[18,19] However, it is difficult to introduce zirconia into mesoporous SBA-15 with high yield because SBA-15 materials are usually synthesized under strong acidic condition.

In this paper, we report a direct-synthesis method for the incorporation of zirconia onto mesoporous SBA-15 under strong acidic condition giving high zirconia content. In the synthesis process, both the zirconia and sulfate source were added to the initial synthesis gel mixture of SBA-15. Because of the introduction of sulfate, a small amount of sulfur exists in the final products (named as SiO_2-SZ). It was found the amount of SO_4^{2-} plays an important role in stabilizing the mesostructure of SBA-15 and tuning the yield of tetragonal zirconia. The catalytic performances of SiO_2-SZ samples are investigated for the esterification of long-chain free fatty acids. Unsupported sulfated zirconia (SZ) is also synthesized to compare its catalytic activity with SiO_2-SZ catalysts to show a higher conversion of free fatty acids for the later.

2. Experimental Section

2.1. Synthesis. A series of mesoporous SiO_2-SZ materials were synthesized using $EO_{20}PO_{70}EO_{20}$ (Pluronic P123, Aldrich) as a template. In a typical synthesis, 1.0 g of P123 was dissolved in 30 mL of H_2O to obtain a clear solution, and 5 mL of 37 wt % HCl (Acros) was added. Then 2.3 mL of tetraethyl orthosilicate (TEOS, Acros) and the required amount of zirconium propoxide (Aldrich, 70%) and ammonium sulfate (Acros) were added. The mixture was stirred for 20 h at 40 °C and further aged at 100 °C for 24 h. The product was collected by filtration, dried, and calcined at 650 °C for 5 h. Samples with different SO_4^{2-}/Zr molar ratio are prepared at a fixed Si/Zr molar ratio of 2, and samples are denoted as $SiO_2-SZ(2, xS)$, where x means the value of the SO_4^{2-}/Zr molar ratio. At a fixed molar ratio SO_4^{2-}/Zr of 1, samples prepared at different Si/Zr molar ratios are denoted as $SiO_2-SZ(y, 1S)$, where y means the value of the Si/Zr molar ratio.

For comparison, a SBA-15 sample was prepared the same way as SiO_2-SZ except that $Zr(OPr)_4$ and $(NH_4)_2SO_4$ were not added. Unsupported sulfated zirconia (SZ) was also prepared by the impregnation method. A total of 5 g of $Zr(NO_3)_4·8 H_2O$ (Acros) was dissolved in 50 mL water, followed by precipitation of zirconium hydroxide at pH 10 using a 5 M NH_3 solution. The resulting $Zr(OH)_4$ was washed with water, impregnated with 1.2 M H_2SO_4, then dried for 10 h at 100 °C, and calcined in air at 650 °C for 5 h.

2.2. Characterization. The powder X-ray diffraction patterns of SiO_2-SZ materials were collected on a Scintag X1 diffractometer using Cu KR (k, 0.1541 nm) radiation. Nitrogen adsorption and desorption isotherms were measured at −196 °C with a Mircomeritics ASAP 2010 instrument. The samples were outgassed for 6 h at 150 °C under vacuum in the degas port of the adsorption analyzer. The specific surface area was calculated with the use of the Brunauer−Emmett−Teller (BET) method. The pore size distributions were obtained by the Barrett−Joyner−Halenda (BJH) method. The total pore volume was calculated at $P/P_0 = 0.91$. Transmission electron microscopy (TEM) micrographs were taken with a Hitachi H-7100 instrument operating at 75∼100 kV or a Philips CM200 at 200 kV. UV−vis diffuse reflectance spectra were measured with a Perkin-Elmer Lambda 18 spectrometer equipped with a Praying-Mantis diffuse reflectance attachment. $BaSO_4$ was used as the reference. Elemental analysis was determined by ICP-mass technique using a Perkin-Elmer Elan-6000 instrument. Sulfur

TABLE 1: Synthesis Conditions and Texture Properties of SiO_2-SZ Calcined at 650 °C

SO_4^{2-}/Zr[a]		Si/Zr[a]		SA$_{BET}$ (m^2/g)	d_{100}[b] (nm)	a_0[c] (nm)	D_p (nm)	T_w[d] (nm)	V_p[e] (cm^3/g)
gel	product	gel	product						
1	0.044	2	3.01	556	10.01	11.56	8.8	2.76	0.85
0.5	0.043	2	3.60	490	10.61	12.25	10.0	2.25	0.98
0.25	0.058	2	6.56	575	10.61	12.25	10.7	1.55	1.25
0	0	2	15.2	628			5.0		0.78
1	0.078	3	5.85	667	9.73	11.24	8.4	2.84	0.94
1	0.063	4	6.74	672	9.91	11.45	8.9	2.55	1.03

[a] Molar ratio. [b] d_{100} calculated from Bragg equation: $2d \sin \theta = n\lambda$ ($\lambda = 0.1541$ nm). [c] $a_0 = 2d_{100}/[graphic1]$. [d] $T_w = a_0 - D_p$. [e] N_2 adsorption volume at $P/P_0 = 0.91$.

analysis was done with a Heraeus VarioEL-III instrument. Temperature-programmed desorption was carried out on a Mircomeritics ASAP 2910 instrument to study acidity of catalysts. In a typical experiment, before NH_3 adsorption, 0.1 g of calcined SiO_2-SZ(2, 1S) sample was pretreated at 400 °C in flowing He for 1 h. The NH_3 adsorption was carried out at 120 °C, and the desorption of NH_3 was started at 120 °C and continued until 600 °C at 10 °C/min.

2.3. Catalytic Studies. Reactions were performed in a stirred batch reactor with samples withdrawn periodically for analysis using an Agilent 6890 gas chromatograph fitted with a 30 m HP-5ms capillary column. Two kinds of fatty acids were used: lauric acid (Acros, 99.5%) and palmitic acid (Sigma, 95%). Anhydrous methyl alcohol (MeOH; Mallickrodr, 99.9%) was used without further purification. The reaction mixtures used in the study had a catalyst/fatty acid/MeOH weight ratio of 2:10:100. Esterification reactions were performed at ∼68 °C, which is the boiling temperature of the reaction mixtures.

3. Results

3.1. Structure and Composition. First, we present the composition and textural properties of the catalyst materials. We will first investigate the effect of varying sulfate loading. Then will fix the sulfate content and study the effect of varying zirconia loading.

Effect of Varying Sulfate Loading. As the initial Si/Zr molar ratio was fixed at 2 in the synthesis process, the influence of sulfate content on the textural properties of sulfated silica−zirconia is shown in Table 1. When no sulfate groups are presented in the synthesis gel, a mixture of SiO_2-ZrO_2 is obtained. Zirconia content in the final product is much lower, and the Si/Zr molar ratio is only 15.20. The Si/Zr molar ratio in the products decreases from 6.6 to 3.0 as the SO_4^{2-}/Zr ratio in the gel is increased from 0.25 to1.0. At first, this seems to be counterintuitive. Zirconium exists as complex ploy-oxo ions in aqueous solution.[20] However, under strong acidic condition, zirconium exists mostly in the cationic form rather than the corresponding polyoxo species. Sulfate groups show a high complexing ability and behave like network formers, bridging different chains together.[21] So zirconium can combine with ammonium sulfate to form the polyoxo ions as $[Zr(OH)_2(SO_4^{2-})_x (H_2O)_y]_n^{n(2-2x)}$. These polyoxo ions can interact strongly with the solution silicate species which are negatively charged under the synthetic condition. The decrease of sulfates in the synthetic gel results in a reduction of zirconium sulfated species formed and thus lowered the zirconia loading in the final product.

Table 1 also lists the SO_4^{2-}/Zr molar ratio in the calcined product. All samples were calcined at the temperature of 650 °C. Although the SO_4^{2-}/Zr molar ratio was high in the gel, only a small amount of sulfur exists in the SiO_2-SZ samples.
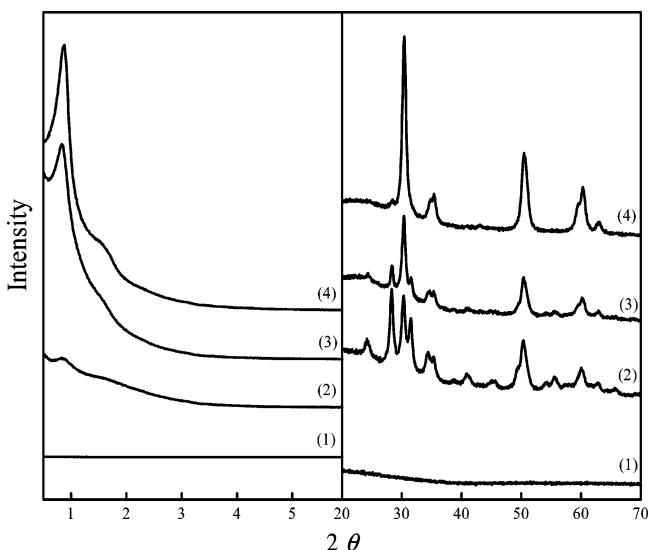
Sulfated Silica-Zirconia Catalysts

J. Phys. Chem. C, Vol. 111, No. 50, 2007 **18733**

Figure 1. XRD patterns of SiO_2−SZ(2, xS) at x = SO_4^{2-}/Zr molar ratios of (1) 0, (2) 0.25, (3) 0.5, and (4) 1. (a) The small angle and (b) the high angle.

Figure 2. Nitrogen adsorption isomerms of SiO_2−SZ(2, xS) at x = SO_4^{2-}/Zr molar ratios of (1) 0, (2) 0.25, (3) 0.5, and (4) 1.

Figure 3. UV−vis DR spectra of SiO_2−SZ(2, xS) at x = SO_4^{2-}/Zr molar ratios of (1) 0, (2) 0.25, (3) 0.5, and (4) 1.

The influence of sulfate content on the structural quality of the SiO_2−SZ can be observed by looking at the (100) reflection in the small angle XRD patterns. From Figure 1a, the XRD patterns of SiO_2−SZ(2, xS) shows that the reduction of gel sulfate content results in a decrease of the intensity of the (100) reflection which means the hexagonal mesostructures are less ordered. At SO_4^{2-}/Zr = 0, no (100) reflection peak is observed in SiO_2−ZrO_2. It indicates the hexagonal mesostructure is not formed at all. Figure 1b also shows the high angle XRD patterns of SiO_2−SZ(2, xS) samples. For SiO_2-SZ(2, 1S), zirconia mainly shows the tetragonal phase, indicated by the main peak at 2θ = 30.2°. Two small peaks of monoclinic zirconia (2θ = 28.5°, 31.5°) appeared in SiO_2−SZ(2, 0.5S). As the ratio of SO_4^{2-}/Zr decreased to 0.25, the intensity of monoclinic zirconia greatly increased suggesting more tetragonal zirconia transformation to monoclinic zirconia. As the ratio of SO_4^{2-}/Zr further decreases to zero, no crystal phases of zirconia are observed. The XRD patterns of SiO_2−ZrO_2(2, 0S) at high angle shown in Figure 1b suggest the sulfate groups favor the formation of well-ordered hexagonal mesostructures and stabilize the tetragonal zirconia.

The N_2 adsorption−desorption isotherms of calcined SiO_2−SZ(2, xS) catalysts (at 650 °C) are shown in Figure 2. At higher gel sulfate content of SO_4^{2-}/Zr = 1 and 0.5, the isotherms exhibit a typical pattern IV according to IUPAC classification and H1-type hysteresis loops. The sharp steps of capillary condensation of N_2 are observed at the relative pressure (p/p_0) of 0.6∼0.8 in the isotherms of SiO_2−SZ(2, 1S) and SiO_2−SZ-(2, 0.5S). For SiO_2−SZ(2, 0.25S) and SiO_2−ZrO_2(2, 0S), the H1-type hysteresis loop becomes more narrow. It is interpreted that the shortened mesopore channels and broadened pore size distributions are presented in the samples of SiO_2−SZ(2, 0.25S) and SiO_2−ZrO_2(2, 0S).

In addition to the nanoparticle form of tetragonal zirconia, some Zr may be incorporated in the framework of silica. UV−visible diffuse reflectance spectroscopy has been successfully used to determine the dispersion of Zr(IV) in the mesoporous silica matrix. It was reported that zirconium-containing mesoporous silica exhibits an absorption peak at 205∼215 nm.[22] In Zr-MCM48, there is an absorption at 207 nm.[23] In both works, the absorption peak near 210 nm is attributed to the ligand-to-metal charge transfer (LMCT) from an O^{2-} to an isolated Zr^{4+}
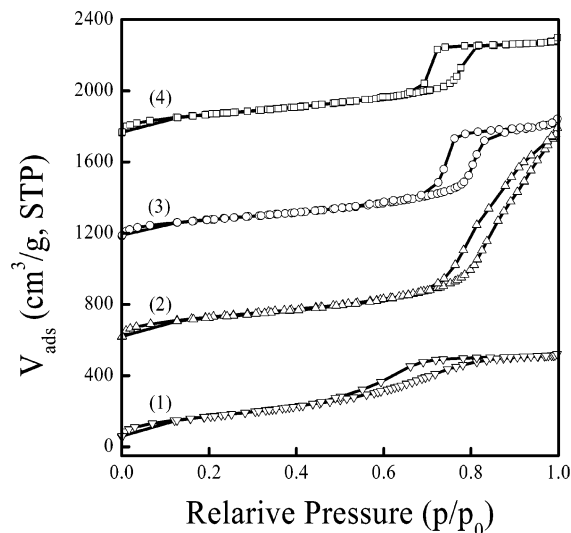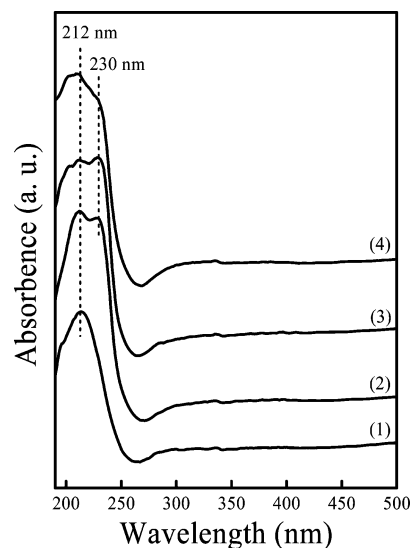
ion in a tetrahedral configuration. ZrO_2 gives an absorption peak at 230 nm, which is assigned to Zr−O−Zr linkage. Figure 3 shows UV−vis spectra of sulfated zirconia-silica samples with various SO_4^{2-}/Zr molar ratio. SiO_2−ZrO_2 without sulfate groups shows only a band at 212 nm, inferring that no crystalline ZrO_2 are detected in the mixture oxides of SiO_2−ZrO_2 and isolated Zr(IV) species are incorporated into the mesoporous silica wall. This result is well in accordance with the high angle XRD pattern for SiO_2−ZrO_2(2, 0S) where no zirconia phase is detected. With the sulfate added to the synthesis gels, SiO_2−SZ(2, xS) samples exhibit two bands at 212 and 230 nm, respectively. These results suggest that some Zr(IV) species are incorporated into the walls of the mesostructured silica in SiO_2−SZ(2, xS) while other Zr(IV) species exist in the tetragonal phase of zirconia(see XRD).

The textural properties of the sulfated silica-zirconia samples are given in Table 1. The pore diameter (D_p) and specific pore volume (V_p) of SiO_2−SZ(2, xS) increase as the SO_4^{2-}/Zr molar ratio is decreased to 0.25. On the other hand, the pore wall thickness (T_w) gradually deceases with lowering of the SO_4^{2-}/Zr molar ratio. All of the calcined products give pore diameters around 10 nm and specific surface area at 500∼600 m^2/g. Table
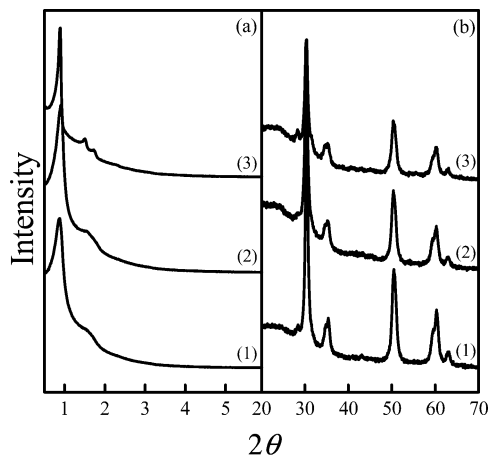
Figure 4. XRD patterns of $SiO_2-SZ(y, 1S)$ at $y = Si/Zr$ molar ratios of (1) 2, (2) 3, and (3) 4. (a) The small angle and (b) the high angle.

1 also shows the zirconium content in the calcined samples: $Si/Zr = 3.01$ for $SO_4^{2-}/Zr = 1$ slightly higher than the Zr yield of $Si/Zr = 3.6$ for $SO_4^{2-}/Zr = 0.5$ and further increases to 6.56 for $SO_4^{2-}/Zr = 0.25$. The change in the Si/Zr molar ratio was investigated at a fixed molar ratio of $SO_4^{2-}/Zr = 1$. From Table 1, the Si/Zr molar ratios of the calcined SiO_2-SZ $(y, 1S)$ products are higher than the Si/Zr molar ratios in the synthesis gels. It is suggested that not all Zr(IV) can form zirconium sulfated polyoxo species under such an acidic condition. As seen in Table 1, increasing Zr content in the synthesis gel also enhances the Zr content in the product. The Si/Zr molar ratio in the calcined sample is 6.74 for $SiO_2-SZ(4, 1S)$, but for SiO_2-$SZ(2, 1S)$, the Si/Zr molar ratio in the calcined sample decreases to 3.01. All of these results suggest that higher molar ratio of SO_4^{2-}/Zr favors more zirconium incorporation onto mesoporous SBA-15 without affecting much the textural properties.

Effect of Changing Si/Zr Ratio. The mesoporous structure of $SiO_2-SZ(y, 1S)$ is characterized in the small angle XRD patterns of Figure 4a. The small angle XRD pattern of calcined $SiO_2-SZ(4, 1S)$ exhibits three well-resolved peaks which are indexed to the (100), (110), and (200) reflections of the 2-D hexagonal *P6mm* structure. As Si/Zr molar ratios are decreased from 4 to 2, the intensity of (100) peaks decreases and the peaks of (110) and (200) are broadened with increasing Zr incorporation. The crystal characteristic of zirconia is exhibited in the high angle XRD patterns of Figure 4b. At a fixed SO_4^{2-}/Zr molar ratio, all of the $SiO_2-SZ(y, 1S)$ samples show peaks characteristic of tetragonal zirconia and the peak widths are gradually increasing with increasing Si/Zr molar ratios.

N_2 adsorption−desorption isotherms of $SiO_2-SZ(y, 1S)$ are shown in Figure 5 and the texture properties are listed in Table 1. All three samples have noticeable hysteresis loops in the type IV isotherms. The surface areas and pore volumes of $SiO_2-$$SZ(y, 1S)$ slightly decrease as the Si/Zr ratio in the synthesis gel is increased. From the small angle XRD patterns and N_2 adsorption−desorption isotherms, $SiO_2-SZ(2, 1S)$ still keeps a well-order mesostructure. It indicates that SiO_2-SZ can be prepared with high Zr loadings while keeping well-ordered mesostructures.

From the UV−visible diffuse reflectance spectra shown in Figure 6, the $SiO_2-SZ(y, 1S)$ samples prepared at different Si/Zr molar ratio are found to have absorptions at 212 and 230 nm, indicating isolated Zr(IV) species in the mesoporous silica wall and nanocrystals of zirconia on mesoporous silica.

Transmission electron micrograph (TEM) of $SiO_2-SZ(2, 1S)$ calcined at 650 °C is shown in Figure 7. Well-ordered channels

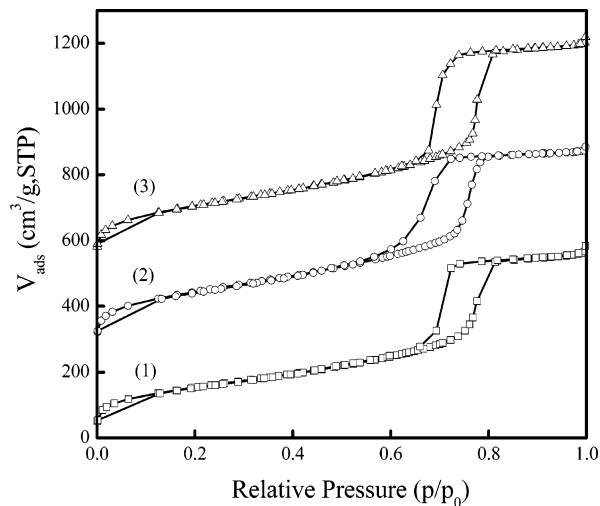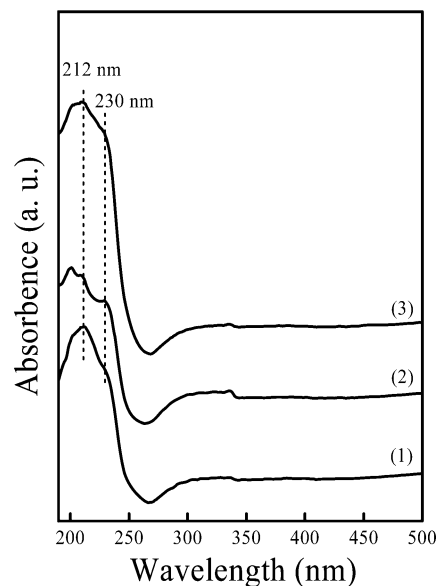**Figure 5.** Nitrogen adsorption isomerms of $SiO_2-SZ(y, 1S)$ at $y = Si/Zr$ molar ratios of (1) 2, (2) 3, and (3) 4.

Figure 6. UV−vis DR spectra of $SiO_2-SZ(y, 1S)$ at $y = Si/Zr$ molar ratios of (1) 2, (2) 3, and (3) 4.

with continuous walls are seen clearly, and zirconia species are obviously scattered into the mesopores. Some zirconia nanoparticles exists outside the channel of mesoporous silica, however.

3.2. Acidity. Acidity of the catalyst was investigated by measuring the temperature-programmed desorption of NH_3. NH_3−TPD profiles of $SiO_2-SZ(2, 1S)$ and unsupported SZ catalysts are shown in Figure 8. Both show broad distributions of acid site strengths. In order to compare the acidity quantitatively, we adjusted same amount of 50 mg of SZ was contained in both catalysts in the experiments. In the case of unsupported SZ, the desorption peak is mainly distributed on the region of 210∼290 °C corresponding to weak acid sites. As zirconia is incorporated onto the mesoporous silica, the intensity of desorption peak was greatly enhanced which means a larger amount acid sites. There is a desorprtion peak at ∼458 °C for $SiO_2-SZ(2, 1S)$, indicating the formation of the strong acid sites. Previously, Lopez et al.[24] measured the acidity of tungstated zirconia by both NH_3- TPD and ion exchange/titration method and concluded that the titration result corroborates better with rates of esterification. Thus, the acidities of the catalysts were also measured by titration with NaOH as
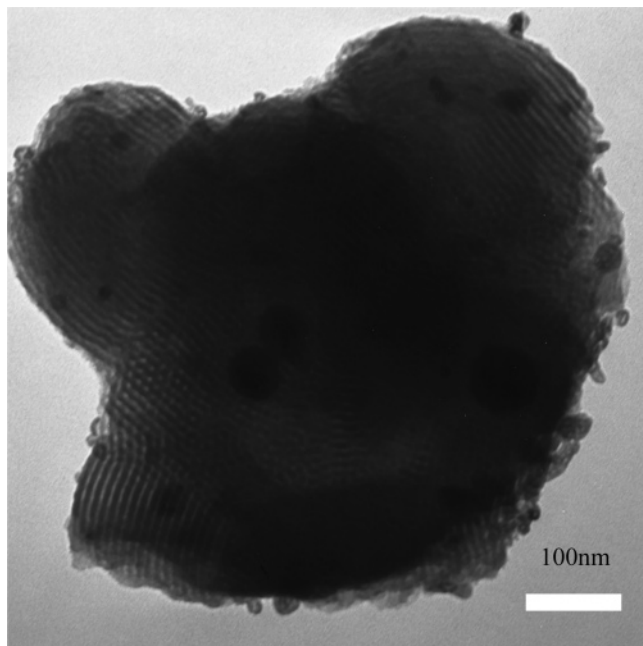
Sulfated Silica-Zirconia Catalysts

J. Phys. Chem. C, Vol. 111, No. 50, 2007 **18735**
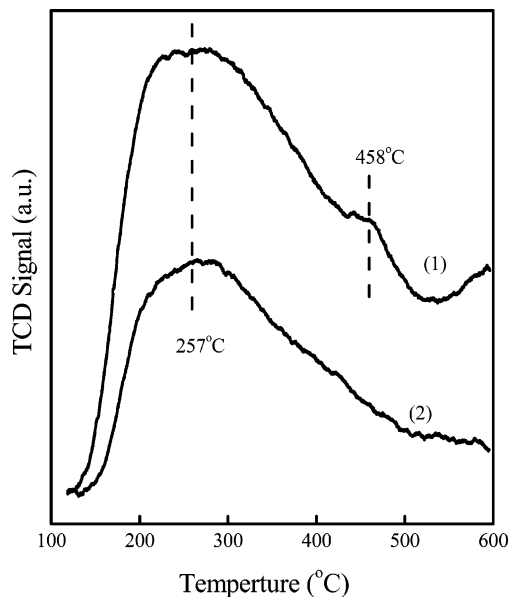
Figure 7. TEM micrograph of the SZ/SBA-15(2, 1S) sample.

Figure 8. NH$_3$ temperature-programmed-desorption profiles of (1) SiO$_2$−SZ(2, 1S) and (2) SZ.

TABLE 2: Acidity by Titration of SiO$_2$−SZ(2,1S) and SZ

catalyst	S/Zr molar ratio	acidity by titration (μmol/g ZrO$_2$)
SiO$_2$−SZ(2,1S)	0.044	1260
SZ	0.15	720

listed in Table 2. An extraordinarily high value of 1260 μmol/g ZrO$_2$ acid sites are detected in SiO$_2$−SZ(2, 1S), much higher than the amount of 720 μmol/g ZrO$_2$ acid sites found in unsupported SZ. This high density of acid sites is comparable with the recently reported very high density of acid sites reported for carbonized glucose.[7b]

3.3. Catalytic Activities. The esterification of long-chain free fatty acids was carried out at 68 °C for 6 h over the direct-synthesis sulfated silica−zirconia, silica−zirconia, and unsupported SZ materials. The conversion results at a reaction time of 6 h are shown in Table 3. For the purpose of comparison, SiO$_2$−SZ(2, 1S) and unsupported SZ were adjusted to contain

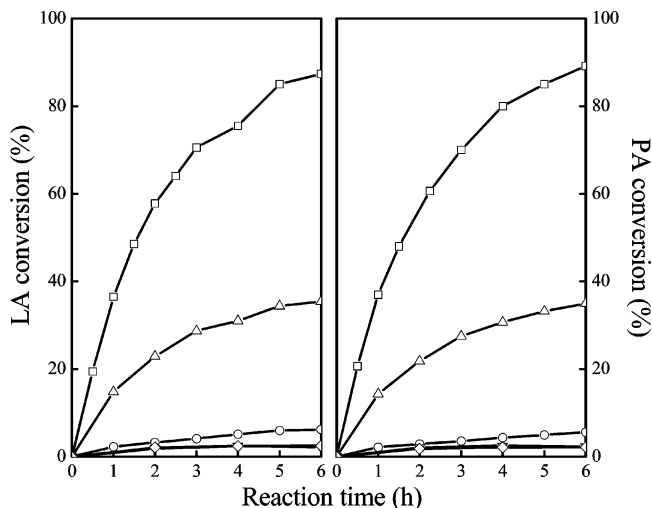**Figure 9.** Catalytic performance of esterification over various catalysts. −□− SiO$_2$−SZ(2, 1S); −○− SiO$_2$−ZrO$_2$(2, 0S); −△− SZ; −▽− SBA-15; −◇− no catalyst.

TABLE 3: Esterification of Fatty Acid with Methanol over SiO$_2$−SZ^a

catalyst	LA conversion (%)	PA conversion (%)
SiO$_2$−SZ(2,1S)	87.4	89.2
SiO$_2$−SZ(2, 0.5S)	38.1	39.4
SiO$_2$−SZ(2, 0.25S)	33.1	33.6
SiO$_2$−ZrO$_2$(2, 0S)	6.20	5.62
SiO$_2$−SZ(3, 1S)	52.1	53.3
SiO$_2$−SZ(4, 1S)	27.0	27.9

^{a} Data obtained after reaction 6 h.

the same amount of sulfated zirconia. The calculated conversion of free fatty acid is based on the 100% selectivity to the fatty acid methyl ester. SiO$_2$−SZ(2, 1S) shows an extraordinarily high catalytic performance with the LA conversion of 87.4% and PA conversion of 89.2%. As one would have expected, increasing the Si/Zr(decreasing Zr loading) decreases the catalytic activity. Lesser sulfation also gives less conversion of fatty acid. SiO$_2$−SZ(2, xS) (x > 0) materials present higher catalytic activity for esterification than SiO$_2$−ZrO$_2$(2, 0S). Unsulfated SiO$_2$−ZrO$_2$(2, 0S) mixed oxides show some weak catalytic activity with the LA conversion of 6.2% and PA conversion of 5.6%. For comparison, the cases of unsupported SZ, pure silica SBA-15 and no catalysts were also examined for the esterification. With no catalyst or with pure silica SBA-15, no activity for the conversion of LA and PA were found. At a reaction time of 6 h, the conversions of LA and PA over unsupported SZ are 35.4% and 35.0%, respectively. Figure 9 shows the time evolution of the conversion of the fatty acids as catalyzed by the solid acids. The reactivities for the two fatty acids, lauric acid and palmitic acid, are very similar showing no chain length effect. Recently, in a study of esterification catalyzed by glucose/H$_2$SO$_4$ derived carbon catalyst,[25] the formation of methyl palmtate, oleate, and stearate gave almost identical rates. There is also no chain length-dependence of activity.

The initial conversions in Figure 9 are quite linear, and we can calculate the initial reaction rates to compare with literature values for other catalysts. The initial rate of methyl laurate (LAME) formation (at 68 °C) is about 175 μmol/min/g cat over SiO$_2$−SZ(2, 1S). In comparison, the initial rate of LAME formation is about 125 μmol/min/g cat over SZ. Methyl palmtate(PAME) gave similar rates. As we have presented in

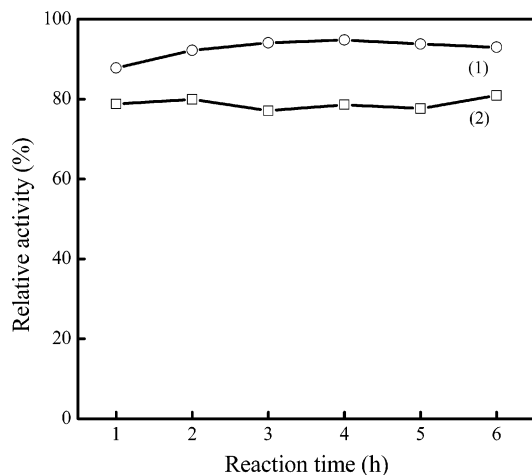**18736** *J. Phys. Chem. C, Vol. 111, No. 50, 2007*

Chen et al.

Figure 10. Effect of water on esterification over (1) SiO_2−$SZ(2, 1S)$ and (2) SZ.

Table 3, the difference in the final conversion at 6 h is even bigger. In a recent study of esterification of methyl oleate formation at 80 °C, Zong et al. found a reaction rate of 143 $\mu mol/min/g$ cat for sulfated zirconia and 478 $\mu mol/min/g$ cat for glucose/H_2SO_4-derived carbon catalyst.[25] Since we are measuring rates at a lower temperature of 68 °C, our SiO_2−SZ catalyst is definitely much more active than sulfated zirconia, niobic acid, amberlyst-15 catalysts reported in ref 25, and probably not far from the excellent glucose-derived catalyst.

To investigate the water effect on the catalytic performance of SiO_2−$SZ(2, 1S)$ and SZ, a small amount of water was added to the mixture of catalysts and reactants at the level of 3600 ppm (weight percent). Under the same reaction conditions, the esterification containing water is compared with the case without adding water. Figure 10 shows the effect of water on the esterification of lauric acid with methanol over SiO_2−$SZ(2, 1S)$ and SZ. The relative activity means the ratio of the conversion of esterification containing 3600 ppm water to the conversion of esterification free of water at the same reaction time. Decreased activities are observed in the water-added esterification for both SiO_2−$SZ(2, 1S)$ and SZ. The relative activity of SiO_2−$SZ(2, 1S)$ is obviously higher than that of SZ, which suggests that SiO_2−$SZ(2, 1S)$ exhibits better tolerance to water.

4. Discussions

The solid acid catalyst system, sulfated zirconia, is rather complex in its acidic site distribution depending on methods of preparation, pretreatments, and type of reactions. Notwithstanding its long history of investigation, we do not yet have a complete understanding of the strong acidity of sulfated zirconia. However, we would like to discuss some possible origins of its excellent catalytic behavior for the esterification reaction. There are several observations we would like to make in this section.

First, we comment on the method of preparation of the catalysts. Previously, in making acid catalysts for alkane isomerization, we used postsynthesis methods of impregnation of sulfated zirconia onto the surface of mesoporous silica.[11] In that method, the resulting zirconia was found to be either nanoparticles or monolayer on the surface of silica. In this paper, we used a direct method of coprecipitation, We found nanoparticles of tetragonal zirconia, but we also have framework incorporation of zirconia. The resulting silica−zirconia materials are weakly acidic, and sulfation creates more surface acidity. Also we note that the mesoporous SBA-15 gives bigger pores (8∼10 nm) and a larger pore volume in contrast to our previous

zirconia supported on MCM-41.[11c] The big pores are necessary for the liquid-state transport of long chain fatty acid.

Second, we would like to discuss the acidity of the solid acid catalysts employed in this work. The esterification reaction of the fatty acid has been shown to be a Brønsted acid-catalyzed reaction.[24] We have measured a higher density of acid site density in the SiO_2−$SZ(2, 1S)$ catalyst than the unsupported sulfated zirconia. It seems there are two sources of the acid sites in the sulfated silica-zirconia materials, one from the nanocrystaline sulfated zirconia itself and the other comes from the mixed silica−zirconia oxides. Rosenberg and co-workers found Brønsted acid sites could be detected on the sulfate-free silica−zirconia mixed oxides by infrared spectroscopic and thermogravimetric techniques.[26,27] These unsulfated materials showed some low activity in the protonation of the C=C group. It would appear that the addition of sulfate leads to the formation of new and stronger Bronsted acid sites on SiO_2−$SZ(2, xS)$ ($x > 0$) materials. On the other hand, in SiO_2−$ZrO_2(2, 0S)$, the crystal phases of zirconia are not observed and the Zr (IV) species are incorporated into the framework of the mesostructured silica, as confirmed by XDR and UV− visible diffuse reflectance spectroscopy. The acid sites are contributed by zirconium (IV) species incorporated in silica. The acidity of SiO_2−$ZrO_2(2, 0S)$ is however weak, so that a small but non-negligible activity could be observed. Isomorphic Zr-substituted mesoporous silicas have been reported previously.[23,28,29] This material shows a relatively low catalytic activity in acid-catalyzed reactions. Upon sulfation, Xiao and co-workers[30] showed that sulfated silica−zirconia exhibits high activities in catalytic cracking of cumene and tri-isopropyl benzene. This material is similar to our sulfated SiO_2−ZrO_2, and their catalytic result seems to agree with our conclusion of higher acidic catalytic activity. Upon high loadings of sulfur and zirconia in the synthesis gel, the tetragonal phase of zirconia would form. It is known that the tetragonal zironia is the catalytically more active form of zirconia.[31] The tetragonal ZrO_2 was formed as sulfate groups are added to the synthesis gel. It is possible that the addition of sulfate may enhance the phase segregation by extracting zirconia to the surface of the mixed oxides and stabilize the tetragonal phase.

Compared to unsupported sulfated zirconia, SiO_2−$SZ(2, 1S)$ exhibits much improved catalytic activity for esterification. As seen in Table 2, the molar ratio of S/Zr in SiO_2−$SZ(2, 1S)$ is 0.044, much lower than the molar ratio of 0.15 of S/Zr presented in unsupported SZ. However, SiO_2−$SZ(2, 1S)$ generates more acid sites (Figure 8 and Table 2) at this lower sulfate density. It is suggested that the high catalytic activity of SiO_2−$SZ(2, 1S)$ did not display the corresponding high sulfate density. Pure silica shows little acidity. However, mesoporous silica as a support can provide high surface area, porosity, and thermal stability.[13,14] SiO_2−$SZ(2, 1S)$ prepared by the direct-synthesis method can facilitate better dispersion of zirconia into the mesoporous silica resulting in a higher number of accessible active sites on the inner surface of the pore wall.

Third, another reason of better performance of SBA-15 supported SiO_2−SZ catalyst is its better tolerance of water. It is known that the pure SBA-15 materials lack acid sites and that the acid sites of SiO_2−$SZ(2, 1S)$ are mainly contributed by sulfated zirconia. Water can inhibit the reaction because it is the product in the esterification of free fatty acid with methanol, shifting the equilibrium toward the reactants.[32] Also water produced may block the acid surface sites. As water is produced in the esterification, the acid sites interacting with water result in a loss of part of the acid sites and lowered its

Sulfated Silica-Zirconia Catalysts

J. Phys. Chem. C, Vol. 111, No. 50, 2007 **18737**

catalytic activity. The lost acid sites of SZ are not recovered in the esterifiction; the conversion was kept at ~78% during the rest of reaction times of 6 h. However, the surface of SBA-15 is quite hydrophilic. For SiO_2−SZ(2, 1S), near the catalytic sites, the neighboring silica surface of SBA-15 can help remove the water produced. Water produced in esterification can be quickly absorbed by the large silica surface. Some acid sited could thus be recovered. The water-addition experiment seems to confirm this conjecture. At the initial stage, parts of the acid sites are covered by water so the relative activity is ~85% at 1 h of reaction time. For a longer reaction time, some water would be excluded from the acid sites by the hydrophilic silica, and the relative activity increases further to ~93%(Figure 10). It is this water-tolerant property of the catalyst that gives a stable catalytic behavior in the esterification reaction.

In conclusion, we have developed a series of mesoporous sulfated silica-zirconia materials as a solid acid catalyst. The materials are shown to possess a higher density of acidic sites in comparison to the unsupported sulfated zirconia. This results in excellent catalytic activity and stability for the esterification of long chain fatty acids.

References and Notes

(1) Lotero, E.; Liu, Y.; Lopez, D. E.; Suwannakarn, K.; Bruce, D. A.; Goodwin, J. G. *Ind. Eng. Chem. Res.* **2005**, *44*, 5353.

(2) Hoydonckx, H. E.; De Vos, D. E.; Chavan, S. A.; Jacobs, P. A. *Top. Catal.* **2004**, *27*, 83.

(3) Kulkarni, M. G.; Gopinath, R.; Meher, L. C.; Dalai, A. K. *Green Chem.* **2006**, *8*, 1056.

(4) Di Serio, M.; Tesser, R.; Dimiccoli, M.; Cammarota, F.; Nastasi, M.; Santacesaria, E. *J. Mol. Catal. A* **2005**, *239*, 111.

(5) Zullaikah, S.; Lai, C. C.; Ramjan, S.; Ju, Y. S. *Bioresour. Technol.* **2005**, *96*, 1889.

(6) Bondioli, P. *Top. Catal.* **2004**, *27*, 77.

(7) (a) Toda, M.; Takagaki, A.; Okamura, M.; Kondo, J. N.; Hayashi, S.; Domen, K.; Hara, M. *Nature* **2005**, *438*, 178. (b) Takagaki, A.; Toda, M.; Okamura, M.; Kondo, J. N.; Hayashi, S.; Domen, K.; Hara, M. *Catal. Today* **2006**, *116*, 157.

(8) Kiss, A. A.; Dimian, A. C.; Rothenberg, G. *Adv. Synth. Catal.* **2006**, *348*, 75.

(9) (a) Mbaraka, I. K.; Shanks, B. H. *J. Catal.* **2005**, *229*, 365. (b) Feng, Y. F.; Yang, X. Y.; Yang, D.; Du, Y. C.; Zhang, Y. L.; Xiao, F. S. *J. Phys. Chem. B* **2006**, *110*, 14142.

(10) Kiss, A. A.; Omata, F.; Dimian, A. C.; Rothenberg, G. *Top. Catal.* **2006**, *40*, 141.

(11) (a) Wang, W.; Chen, C. L.; Xu, N. P.; Mou, C. Y. *Green Chem.* **2002**, *4*, 257. (b) Chen, C. L.; Cheng, S. F.; Lin, H. P.; Wong, S. T.; Mou, C. Y. *Appl. Catal. A* **2001**, *215*, 21. (c) Chen, C. L.; Li, T.; Cheng, S. F.; Lin, H. P.; Bhongale, C. J.; Mou, C. Y. *Microporous Mesoporous Mater.* **2001**, 201.

(12) Mbaraka, I. K.; Radu, D. R.; Lin, V. S.; Shanks, B. H. *J. Catal.* **2003**, *219*, 365.

(13) Liu, Y.; Lotero, E.; Goodwin, J. G. *J. Catal.* **2006**, *243*, 221.

(14) (a) Zhao, D.; Feng, J.; Huo, Q.; Nelosh, N.; Fredrikson, G.; Chmelka, B. F.; Stucky, G. D. *Science* **1998**, *120*, 278. (b) Zhao, D.; Huo, Q.; Feng, J.; Chmelka, B. F.; Stucky, G. D. *J. Am. Chem. Soc.* **1998**, *120*, 6024.

(15) Li, T.; Wong, S. T.; Chao, M. C.; Lin, H. P.; Mou, C. Y.; Cheng, S. *Appl. Catal. A* **2004**, *261*, 211.

(16) Wang, J. H.; Mou, C. Y. *Appl. Catal. A* **2005**, *286*, 128.

(17) Landau, M. V.; Titelman, L.; Vradman, L.; Wilson, P. *Chem. Commun.* **2004**, *24*, 594.

(18) Selvaraj, M.; Lee, T. G. *J. Phys. Chem. B* **2006**, *110*, 21793.

(19) Vinu, A.; Sirnivasu, P.; Miyahara, M.; Ariga, K. *J. Phys. Chem. B* **2006**, *110*, 801.

(20) El Brahimi, M.; Durand, J.; Cot, L. *Eur. J. Solid State Inorg. Chem.* **1988**, *25*, 185.

(21) Ciesla, U.; Fröba, M.; Stucky, G.; Schüth, F. *Chem. Mater.* **1999**, *11*, 227.

(22) Tuel, A.; Gontie, S.; Teissier, R. *Chem. Commun.* **1996**, *5*, 651.

(23) Morey, M. S.; Stucky, G. D.; Schwarz, S.; Fröba, M. *J. Phys. Chem. B* **1999**, *103*, 2037.

(24) Lopez, D. E.; Suwannakarn, K.; Bruce, D. A.; Goodwin, J. G. *J. Catal.* **2007**, *247*, 43.

(25) Zong, M. H.; Duan, Z. Q.; Lou, W. Y.; Smith, T. J.; Wu, H. *Green Chem.* **2007**, *9*, 434.

(26) Rosenberg, D. J.; Anderson, J. A. *Catal. Lett.* **2002**, *83*, 59.

(27) Rosenberg, D. J.; Bachiller-Baeza, B.; Dines, T. J.; Anderson, J. A. *J. Phys. Chem. B* **2003**, *107*, 6526.

(28) Chen, S. Y.; Jang, L. Y.; Cheng, S. F. *Chem. Mater.* **2004**, *16*, 4174.

(29) Chao, M. C.; Lin, H. P.; Mou, C. Y.; Cheng, B. W.; Cheng, C. F. *Catal. Today* **2004**, *97*, 81.

(30) Du, Y. C.; Sun, Y. Y.; Di, Y.; Zhao, L.; Liu, S.; Xiao, F. S. *J. Porous Mater.* **2006**, *13*, 163.

(31) Morterra, C.; Cerrato, G.; Ardizzone, B.; Bianchi, C. L.; Signoretto, M.; Pinna, F. *Phys. Chem. Chem. Phys.* **2002**, *4*, 3136.

(32) (a) Liu, Y.; Lotero, E.; Goodwin, J. G. *J. Catal.* **2006**, *242*, 187. (b) Liu, Y.; Lotero, E.; Goodwin, J. G. *J. Mol. Catal. A* **2005**, *245*, 132.